ELSEVIER

PII: S0032-3861(97)10067-2

Polymer Vol. 39 No. 15, pp. 3411–3416, 1998

0032-3861/98/$19.00+0.00

Poly(ether imide) membranes obtained from solution in cosolvent mixtures

K.-V. Peinemann[a], J. F. Maggioni[b] and S. P. Nunes[b,*]
[a]*GKSS-Forschungszentrum, 21502 Geesthacht, Germany*
[b]*University of Campinas, 13083-940 Campinas, Brazil*
(Received 28 May 1997; revised 25 July 1997)

Integral asymmetric membranes for gas separation were prepared by casting a poly(ether imide) solution in tetrahydrofuran (THF) and gamma-butyrolactone (GBL) and coagulating in water. As observed by electron microscopy, very thin selective layers ($< 0.5\ \mu m$) were obtained with high GBL contents or when butanol was also added to the casting solution, resulting therefore in the highest permeability values (up to 467 l He/m^2 h bar for membranes prepared from casting solutions with 56 wt% GBL). He/N_2 selectivity values as a function of solvent composition went through a maximum. Maximum values as high as 131 were obtained with equal amounts of THF and GBL in the solvent mixture. The kinetics and mechanism of membrane formation were investigated by light scattering. © 1998 Elsevier Science Ltd. All rights reserved.

(Keywords: phase separation; spinodal decomposition; nucleation and growth)

INTRODUCTION

Poly(ether imide) (PEI) has been successfully used in the preparation of asymmetric porous membranes for gas separation[1,2]. PEI membranes have an unusually high He selectivity compared to other commercial polymers combined with a reasonable He permeability. As for most asymmetric membranes, they are prepared by phase inversion[3,4], the polymer solution being cast on a substrate and immersed in a non-solvent bath. However, to attend the requirement of very thin top layers, the best results have been obtained by addition of non-solvents to the casting solution[2,5]. By this procedure, a homogeneous casting solution is still obtained but the thermodynamic condition is very near the phase separation. Due to a very fast evaporation of one of the solvent components, the solution may start demixing even before immersion in the coagulation bath. Having this principle in mind, membranes with high selectivity for He/N_2 (*ca.* 220) and He flux of 0.2 m^3/m^2 h bar have been prepared[1] with thin dense top layers (about 0.1 μm thick) using the following casting solution coagulated in acetone: PEI dissolved in a mixture of dichloromethane (very volatile solvent), 1,1,2-trichloroethane (solvent), xylene (non-solvent) and acetic acid (non-solvent). Their good performance was confirmed in pilot plants (capacity 100 m^3/h) for recovering helium from diving gas[2]. However, the requirement of solvents like trichloroethane and xylene for the casting solution and large amounts of acetone for the coagulation bath made the preparation process unviable for large scale production. To obtain membranes with similar performance but avoid eventual environmental problems, in this work a new process for preparation of gas separation membranes from poly(ether imide) solutions coagulated in water is described. Tetrahydrofuran and gamma-butyrolactone are both non-solvents for poly(ether imide). However, when mixed in suitable proportions a solution is obtained and the new solvent mixture for poly(ether imide) provides membranes with thin selective layers and a wide variety of microporous structures. The cosolvence itself is quite interesting from the thermodynamic point of view and will be discussed in further papers. Here the permselectivity and morphology of membranes obtained from THF/GBL/PEI are analysed and some aspects of the mechanism of membrane formation are discussed.

* To whom correspondence should be addressed at: GKSS-Forschungszentrum, 21502 Geesthacht, Germany

EXPERIMENTAL

Poly(ether imide) ULTEM 1000 was supplied by General Electric.

Membrane preparation

Polymer solutions containing PEI, THF and GBL were cast on a polypropylene non-woven in a continuous machine, forming 150 μm thick films, which were coagulated in water at 18°C. The membranes were then washed during some hours in water and dried at 90°C. The polymer concentration in solution was always around 15.5 wt%, which had a convenient viscosity for casting. In some cases also n-butanol was added to the casting solution.

Membranes which should be tested for gas separation were further coated with a 3 wt% Elastosil E41 Wacker silicone solution in petroleum benzine (boiling range 40–60°C). The coating minimized the effect of eventual defects on the membrane surface.

Gas permeation

The permeation of N_2 and He through the membrane obtained from different casting solutions was measured by standard procedures[6].

Morphology

The morphology of membranes prepared in the machine was analysed by scanning electron microscopy. They were fractured in liquid nitrogen, coated with chromium and observed in a JSM 6400-F JEOL field emission scanning electron microscope.

Membranes prepared in the machine were practically immediately (after about 3–6 s) immersed in water after casting. In order to investigate the effect of solvent evaporation on the morphology, polymer solutions were cast in films also with initial thickness of *ca.* 150 μm on glass and immersed in water in a similar condition to that used in the machine, but different evaporation times (10 s and 10 min) before coagulation.

Light scattering measurements

Fundamental aspects. Light scattering has been widely used for investigation of the mechanism of phase separation in polymer systems[7–9] and has also been shown to be a useful tool for membranes[10]. The theory has been described in detail elsewhere[7,8,10] and will be only briefly reviewed here.

During membrane formation, phase separation is induced to promote the pore formation. In systems containing only amorphous polymers such as poly(ether imide), the contribution of solid–liquid demixing (crystallization) can be disregarded. Two mechanisms of liquid–liquid demixing may predominate: nucleation and growth (NG) and spinodal decomposition (SD). When phase separation takes place by nucleation and growth, it initiates with the formation of nuclei of a polymer diluted phase dispersed in a concentrated polymer matrix. The growing nuclei give rise to the membrane pores. Light going through the system is scattered and a monotonic decrease of scattered light intensity with angle is normally observed[7]. At a fixed angle, the intensity of scattered light, I, as a function of time, t, can be fitted to a power law, $\log I$ *versus* $\log t$ being a straight line.

On the other hand, if spinodal decomposition predominates, concentration fluctuations with characteristic wavenumbers, q, start to grow, leading to two continuous phases. A structure with high periodicity characterizes the system at least in its early stages of phase separation. Light going through such a film is scattered, producing a typical diffraction halo. Changes in this pattern follow the linear Cahn theory[11]:

(i) the scattered light intensity, I, *versus* angle, θ, or *versus* q [$q = (4\pi/\lambda)\sin(\theta/2)$], should go through a maximum;
(ii) at a constant angle, the intensity of scattered light, I, should exponentially increase with time (linear $\ln I$ *versus* t plots);
(iii) the slope of a $\ln I$ *versus* t plot at a fixed angle gives $2R(q)$, the growth rate of fluctuations with wavenumber q. In systems with spinodal decomposition, plots of $R(q)/q^2$ *versus* q^2 are linear and the extrapolation to $q = 0$ allows an estimation of the apparent diffusion coefficient, D_{app}. D_{app} expresses how fast the phase separation takes place. D_{app} depends both on thermodynamic and kinetic aspects. From the kinetic point of view, it is larger in systems with high mobility. From the thermodynamic point of view, the phase separation is faster far from the spinodal curve, inside the two phases region of the phase diagram. $D_{app} = 0$ very near the spinodal curve.

Experimental set. The mechanism of pore formation in the membranes was investigated here using a diode array for light scattering measurements at different angles. A device for very fast acquisition was necessary. The system described in *Figure 1* was mounted in the laboratory on an optical bank. A He–Ne laser (633 nm), 10 mW, was used as light source. A diode array produced by Cronic Electronic, with a total length of 26 mm, containing 1024 elements, separated from each other by 25 μm, was placed as detector, orthogonally to the laser beam and connected to a 486 computer by an interface card. The total range of angles covered by the detector could be adjusted, by moving the diode array in relation to the sample. For the experiments described here, the diode array was positioned at about 2.5 cm above the sample, allowing simultaneous measurements of the light scattered by the sample in angles from 0 up to *ca.* 40 (covered by a total of 1024 points). Software permitted the acquisition of a series of 24 integrated measurements (with 1024 points each), separated by time intervals of 0.5 s. The period during which the signal for each measurement was accumulated (integrated) could also be adjusted, and 15 ms was typically chosen for that, being long enough to allow a good detection of the scattered light. For the choice of this parameter, it was also taken into account that the period should be short enough to avoid detector saturation. For the same reason, the experiment was performed in a dark room. The acquisition period was also short enough to discard any contribution due to disturbances in the coagulation bath. Measurements without the polymer film were previously performed to confirm that no disturbance would affect the scattered light detection.

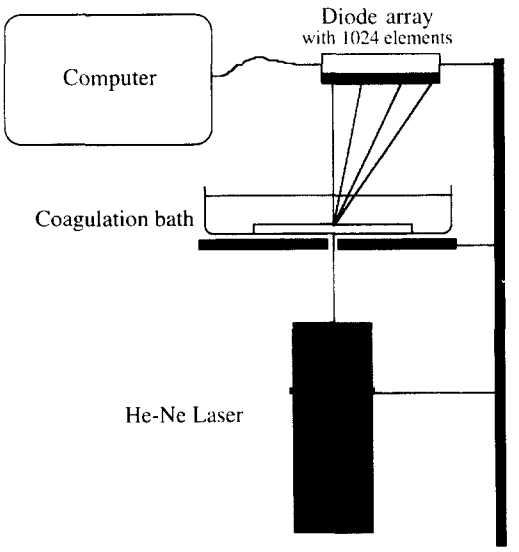

Figure 1 Experimental system for light scattering measurements

For the measurements, a thin layer of polymer solution was cast on a glass normally used as sample holders for optical microscopy. The sample was located between the laser and the diode array. Demixing was then promoted in two different ways: (i) by evaporation of the more volatile solvent, THF; and (ii) by immersion in a coagulation bath. In this case, the sample was immersed in a Petri dish containing water. The detection was simultaneously started by pressing a key of the computer keyboard and 24 consecutive measurements were automatically recorded.

RESULTS AND DISCUSSION

With a constant PEI content, changing the THF/GBL proportions, completely different characteristics of gas flux and selectivity can be achieved, as shown in *Table 1*.

With high THF contents a very low gas flux is measured, compromising the viability of the membranes. One reason for that is the thickness of the selective layer as evidenced by the morphological investigation. All the membranes in

Table 1 Gas flow and selectivity of membranes obtained from 15.5 wt% PEI casting solutions with different solvent compositions

THF/GBL/butanol content (wt%)	Gas flux[a] (l/m^2 h bar)		Selectivity[a] He/N_2
	N_2	He	
28.5/56/0	18 ± 1	467 ± 40	26 ± 2
34.2/50.4/0	6 ± 2	397 ± 62	74 ± 34
42.3/42.3/0	2.5 ± 0.9	295 ± 29	131 ± 42
56.0/28.5/0	0.2 ± 0.1	7.5 ± 0.7	37 ± 14
53.0/28.5/3	2.9 ± 0.4	265 ± 34	94 ± 17

[a] Average from *ca.* five values

Table 1 were formed in the machine by coagulation in water. Immersion was promoted about 3–6 s after casting. Eventual influences of solvent evaporation during this short period, solvent exchange and/or the mechanism of pore formation are discussed below. The gas flux increases monotonically both for He and N_2 as the GBL content increases. But the most remarkable change occurs in the membrane selectivity. A maximum is observed when the THF and GBL contents are equal. Higher GBL contents may lead to even thinner selective layers, but with more incidence of defects. An effect similar to that observed when increasing the GBL content could also be seen by adding some butanol to the casting solution.

From electron microscopy, two different structures were observed from the top to the bottom of the membrane, as shown in *Figures 2 and 3*. The thickness of the top layer was

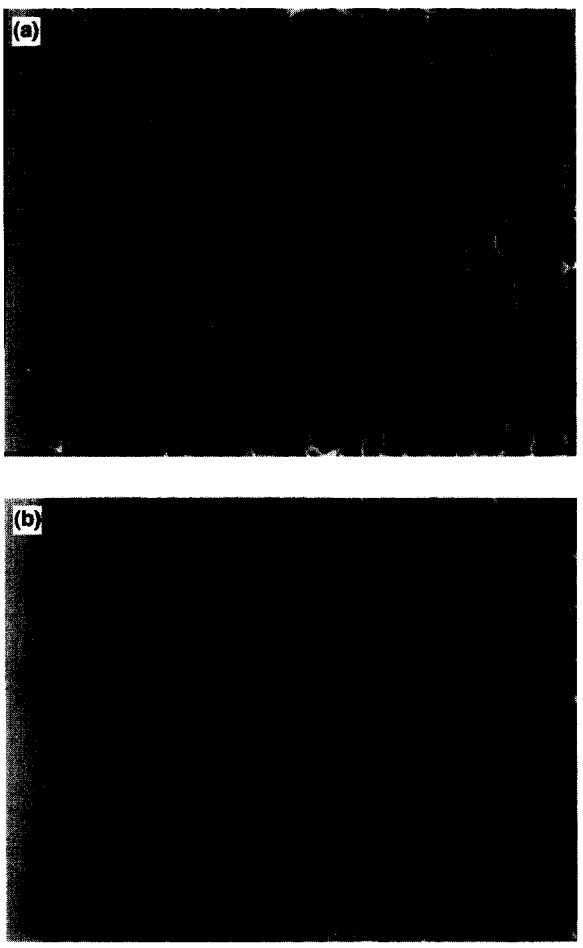

Figure 2 Scanning electron microscopy of membranes obtained after immersion in water of 15.5 wt% PEI casting solutions with the following solvent composition: (a) 56% THF and 28.5% GBL; (b) 54% THF, 28% GBL and 3% butanol. Solvent evaporation period 10 s

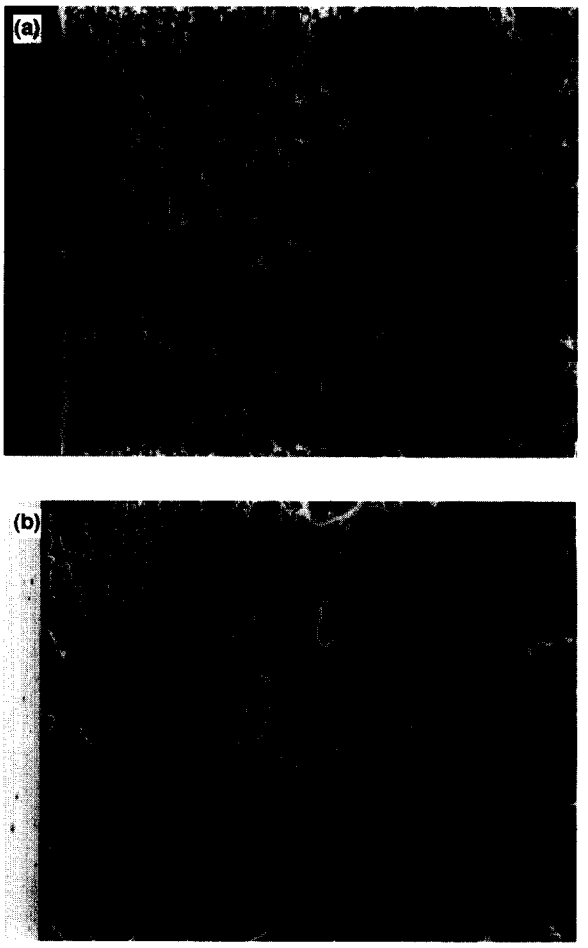

Figure 3 Scanning electron microscopy of membranes obtained after immersion in water of 15.5 wt% PEI casting solutions containing 28 wt% THF and 56 wt% GBL. Solvent evaporation periods: (a) 10 s and (b) 10 minutes

estimated for membranes obtained with different times of solvent evaporation before immersion in water, as shown in *Table 2*. It increased as the evaporation time increased, as also shown in *Figure 3*. In any case the thickness of the top layer was clearly a function of the solvent composition, membranes with higher THF content having a thicker top layer. Casting solutions with butanol led to a thinner top layer.

From light scattering experiments it was possible to detect the time to start the phase separation. In *Table 2*, the values followed by '(air)' correspond to experiments for which phase separation was promoted only by solvent evaporation, while those followed by '(water)' correspond to phase separation induced by immersion in water. Solutions containing 3 wt% butanol start demixing induced by solvent evaporation very fast (less than 1 s). Therefore, during membrane preparation, the top layer is formed by phase separation starting before immersion in water. In contrast, casting solutions with similar THF/GBL/PEI composition, but without butanol, start demixing after 40 s of solvent evaporation. In membranes prepared from these solutions, the top layer is therefore exclusively formed by solvent–water exchange.

The pore formation in membranes has been a topic of fruitful discussion in the literature[3,4,10,12,13]. To understand the formation of the top layer, it is very important to know not only how long it takes to start phase separation, but how fast it takes place, which mechanism it follows and when it can be stopped.

Table 2 Membranes obtained by casting a 15.5 wt% PEI solution containing THF/GBL/n-butanol

Solvent composition (wt%) THF/GBL/ butanol	Electron microscopy			Light scattering	
	Top layer thickness (μm)			Time to start phase separation (s)	Time to start gelation (s)
	Evaporation time				
	Machine	10 s	10 min		
56.0/28.5/0	2.5	6.4	18.4	40 (air)	46.5 (air)
				1.5–2 (water)	3.2 (water)
55.0/28.5/1.4		4.6	10	8 (air)	10.5 (air)
				1 (water)	2.0 (water)
53.0/28.5/3.0	0.5	1.4	10	0.7 (air)	1.2 (air)
				0.2 (water)	0.4 (water)
42.3/42.3/0	1.0			6.5 (air)	10.0 (air)
				1 (water)	1.2 (water)
28.0/56.0/0	< 0.1	< 0.1	6	6 (air)	11.0 (air)
				0.2 (water)	0.5 (water)

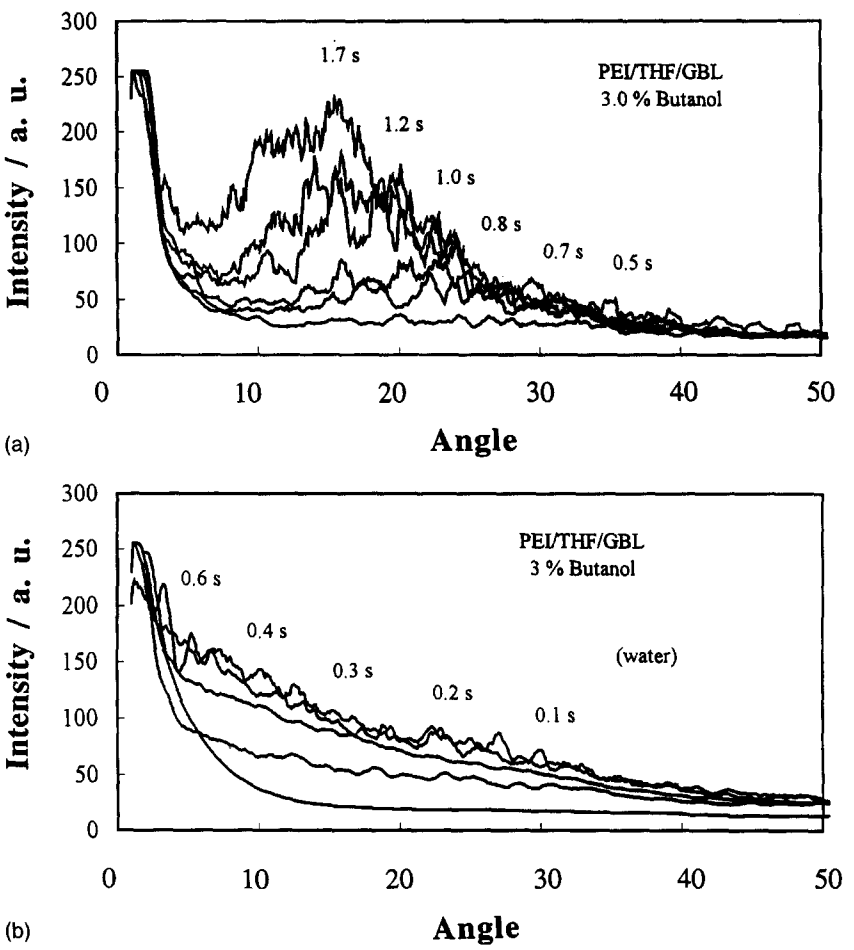

Figure 4 Light scattering as a function of scattering angle (°) in different times for 15.5 wt% PEI solutions containing 54 wt% THF, 28 wt% GBL and 3 wt% n-butanol. Phase separation induced by (a) solvent evaporation (spinodal decomposition) and (b) immersion in water (nucleation and growth)

Light scattering is a useful tool to investigate the mechanisms of phase separation in polymer systems. The formation of a porous structure in an asymmetric membrane is a complex process. During solvent evaporation and immersion in water, the composition is continuously changing across the nascent membrane film and the thermodynamic condition for phase separation is not simultaneously attended all over the film. Different mechanisms may be favoured in different regions of a nascent membrane resulting from the same homogeneous starting solution. The experiments described here give information on the first phase separation steps detected in the film and therefore correspond to the formation of the top layer. *Figure 4a* and *b* show examples of light intensity as a function of scattered angle curves recorded after consecutive times for systems demixing by (a) spinodal decomposition and (b) nucleation and growth.

Values of ln I were plotted as a function of time for films

with different compositions during demixing, as shown in *Figure 5*.

According to criteria mentioned above, the mechanism of phase separation could be identified and, in case of systems for which spinodal decomposition predominated, linear $R(q)/q^2$ *versus* q^2 plots were obtained as shown in *Figure 6*.

Values of D_{app} were calculated, indicating how fast phase separation took place. Here again two kinds of experiments were performed: (i) phase separation induced by solvent evaporation ('air') and phase separation induced by immediate immersion in water ('water'). The results are summarized in *Table 3*. From those following SD, D_{app} is clearly larger for solutions containing 3 wt% butanol. In this case, not only phase separation starts much earlier, as seen in *Table 2*, but the spinodal decomposition also evolves much faster.

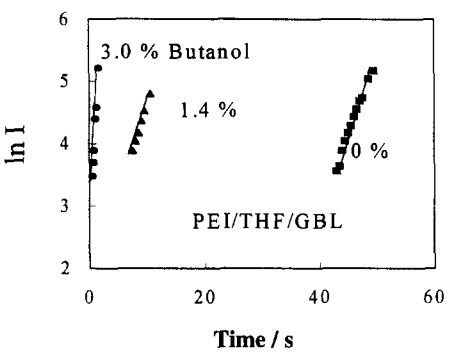

Figure 5 Logarithmic plot of scattering light intensity as a function of time for 15.5 wt% PEI solutions containing (■) 56.0/28.5/0, (▲) 55.0/28.5/1.4 and (●) 53.0/28.5/3.0 weight per cent THF/GBL/n-butanol during solvent evaporation ($q = 2.3\ \mu m^{-1}$)

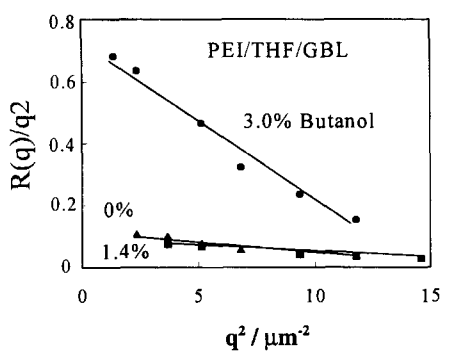

Figure 6 Plots of $R(q)/q^2$ as a function of q^2 for 15.5 wt% PEI solutions containing (▲) 56.0/28.5/0, (■) 55.0/28.5/1.4 and (●) 53.0/28.5/3.0 weight per cent THF/GBL/n-butanol during solvent evaporation

Table 3 Light scattering investigation of mechanism of phase separation in membranes obtained from 15.5 wt% PEI casting solutions containing THF/GBL/n-butanol

Solvent composition (wt%) THF/GBL/butanol		Mechanism of phase separation	D_{app} ($\mu m^2\ s^{-1}$)	q_m (μm^{-1})
56.0/28.5/0	(air)	SD	0.12	5–2
	(water)	SD	0.10	12
55.0/28.5/1.4	(air)	SD	0.09	5
	(water)	NG		
53.0/28.5/3.0	(air)	SD	0.71	5
	(water)	NG		
42.3/42.3/0	(air)	SD	0.20	2
	(water)	NG		
28.0/56.0/0	(air)	SD	0.10	9
	(water)	NG		

In most of the cases, for the same casting solution, different mechanisms of phase separation predominate when induced by solvent evaporation or by immersion in water. In many cases the formation of the top layer starts before immersion in water and the coarser porous structure below it begins to be formed after immersion. Different mechanisms could be involved in the different patterns of morphology which can be seen across the membrane. If only the early stages of phase separation were to be taken into account, spinodal decomposition should favour interconnected pores, while nucleation and growth should favour a closed cell porous structure. However, by both phase separation mechanisms, in later stages[14], the phases may coalesce to form a coarser structure, as can be seen in *Figure 3*. Morphology alone should therefore not be used as evidence to differentiate mechanisms of phase separation.

q_m values are the wavenumbers of the predominant concentration fluctuation in the system. $2\pi/q_m$ is the periodic distance between the continuous phases resulting from the fluctuations. At least in the early stages of phase separation, this distance is constant. The interphase distance remains constant during phase separation in almost all the systems. In membranes the dilute phase gives rise to the pores, while the polymer concentrated phase forms the membrane matrix. If the morphology is frozen and is not allowed to change any more, $2\pi/q_m$ gives information on the relative pore size in the top layer. Only in solutions with higher THF content and no butanol was a shift of q_m to lower values observed, indicating that phase coalescence occurs before the morphology is fixed.

As already mentioned, coalescence may follow both NG or SD, leading to a coarser structure. Even more important than the mechanism of phase separation is therefore the possibility of stopping demixing at a convenient stage and freezing the resulting structures to form a suitable membrane. During membrane formation, one of the separating phases is a polymer concentrated matrix. If the viscosity of this concentrated phase is high enough, the phase separation is slowed down and stopped. The morphology is practically frozen. This decrease of system mobility and consequent 'slowing down' of the phase separation process will be referred to here as 'gelation'. Gelation was detected as a change of slope in $\ln I$ *versus* t plots (for systems following SD mechanism) or in $\log I$ *versus* $\log t$ plots (for systems following NG). The time preceding gelation is also shown in *Table 2* for different experiments. Gelation starts much faster in systems with 3 wt% butanol. The morphology of the top layer is fixed just 0.5 s after demixing starts due to solvent evaporation. Therefore, even before immersion in water, a thin top layer with low mobility has already been established. In water, the porous structure below it is further formed by solvent–water exchange, but the top layer is not altered any more. Without butanol, in systems with high THF content, gelation starts much later after immersion in water. During a longer period (up to 2 s), the top layer mobility remains high during solvent–water exchange. Phase separation proceeds and a thick top layer is formed before the morphology can be fixed. In systems without butanol, but with high GBL content, phase separation starts probably just before immersion in water. The time required to start demixing induced by solvent evaporation is about the time between casting and immersion in the machine. When immersed in water, gelation starts very fast, fixing the morphology with a very thin top layer.

ACKNOWLEDGEMENTS

The authors thank FAPESP for financial support.

REFERENCES

1. Peinemann, K.-V., Verfahren zur Herstellung einer integral-asymmetrischen Membran. Deutsche Patentschrift DE 3420373, 1986.
2. Peinemann, K.-V., Ohlrogge, K. and Knauth, H.-D., The recovery of helium from diving gas with membranes, in *Membranes in Gas Separation and Enrichment*. Special publication No. 62, Royal Society of Chemistry, London, 1986, pp. 329–341.
3. Kesting, R., *Synthetic Polymeric Membrane*. Wiley, New York, 1985.
4. Mulder, M., *Basic Principles of Membrane Technology*. Kluwer Academic, The Netherlands, 1991.
5. Peinemann, K.-V., Wind, J. and Aderhold, M., Ultrathin polyetherimide membranes for gas separation. *7th Int. Symp. on Synthetic Membranes*, Tübingen, September 1994.
6. Jia, M.-D., Peinemann, K.-V. and Behling, R.-D., *Ceramic zeolite composite membranes. J. Membr. Sci.*, 1993, **82**, 15–26.
7. Hashimoto, T., in *Current Topics in Polymer Science*, Vol. II, eds. R. M. Ottenbrite, L. A. Utracki and S. Inoue. Hanser, Munich, 1987, pp. 199–242.
8. Inoue, T. and Ougizawa, T., *Characterization of phase behavior in polymer blends by light scattering. J. Macromol. Sci. Chem.*, 1989, **A26**, 147–173.
9. Silveira, K. F., Yoshida, I. V. and Nunes, S. P., *Phase separation in PMMA/silica sol–gel systems. Polymer*, 1995, **36**, 1425–1434.
10. Nunes, S. P. and Inoue, T., *Evidence for spinodal decomposition and nucleation and growth mechanisms during membrane formation. J. Membr. Sci.*, 1996, **111**, 93.
11. Cahn, J. W., *J. Chem. Phys.*, 1965, **42**, 93–99.
12. Koros, W. J. and Pinnau, I., Membrane formation for gas separation processes, in *Polymeric Gas Separation Membranes*, eds. D. R. Paul and Y. Yampol'skii. CRC Press, Boca Raton, FL, 1994, pp. 209–271.
13. van den Boomgaard, Th., Boom, R. M. and Smolders, C. A., *Diffusion and phase separation in polymer solution during asymmetric membrane formation. Makromol. Chem., Macromol. Symp.*, 1990, **39**, 271–281.
14. Siggia, E. D., *Late stages of spinodal decomposition in binary mixtures. Phys. Rev. A*, 1979, **20**, 595–605.